Understanding Fivefold Symmetry in Electron-Diffraction Patterns

Lequan Min

School of Mathematics and Physics
University of Science and Technology Beijing, Beijing 100083, PR China

Abstract

Electron-diffraction patterns with 5-fold rotational symmetry of experimental alloy phases are assumed to be produced by periodic structures. A three-dimensional periodic structures is presented based on two kind polyhedrons. These structures can be used as an atomic model to describe the alloy phases. The Fourier-transform patterns of the models are found to be similar to the corresponding electron-diffraction patterns of these alloy phases along three "symmetry directions". Details of the motivations and approaches that lead to these models are discussed.
Keywords: Condensed matter physics; Electron-diffraction; 5-fold symmetry; Quasicrystal; Two kind polyhedrons; Periodic model; Fourier-transform patterns.

1 Introduction

According to the classical crystallographic theory, a crystal structure can have n-fold rotational symmetry only if n = 2, 3, 4, or 6. As a consequence, the diffraction patterns of a crystal structure have only the same n-fold symmetry. The discoveries of the alloy phases with 5−, 8−, 10−, and 12−fold symmetry electron-diffraction patterns (EDPs) consisting of sharp peaks [see [1, 2, 3, 4, 5]] have broken the crystallographic restriction.

The popular point of view is that these alloy phases are a fundamentally new class of ordered atomic structures that exhibit: long-range quasiperiodic translation order, and long-range orientational order with disallowed crystallographic symmetry; or practically these phases are randomly packed (see [6]). These phases are now called quasicrystals.

The EDPs show 12-fold rotational symmetry were observed by Chen Li, and Kuo[5] in V-Ni and V-Ni-Si alloys in 1988. The group have interpreted their alloys as two-dimensional quasicrystals rather than crystals. In previous papers ([7, 8, 9]), we introduced several 3D periodic structures based on so-called $T - polyhedron$. These structures have be used as mathematical models to describe the V-Ni and V-Ni-Si alloy systems. The Fourier-transform patterns (FTPs) of the models were in good agreement with all of the corresponding EDPs of these alloys.

In a previous version of this study[10], we have reported that the high-resolution electron-microscopic (HREM) image of Mn-Al-Si taken with the incident beam parallel to the fivefold symmetry zone axis cannot be described by Penrose tiling [see Fig. 3 in Ref. [11]]; the HREM image has periodic characteristic formed by isolated and embedded regular pentagonal dodecahedrons. The positions of the sports of the EDP shown 5-fold rotational symmetry can be assumed to located at integral lattice points in orthogonal coordinate system. We have presented two three-dimensional periodic models based on regular pentagonal dodecahedrons to describe the quasicrystals with 5-fold symmetry EDPs.

In this study, we will present a improves periodic model. The fundamental units of the model consist of two kind polyhedrons: (a) Regular icosahedron without vertices at top and bottom(RIWV). (b) Polyhedron with a pentagon at both the top and bottom, and isosceles triangle as its lateral (PPIT).

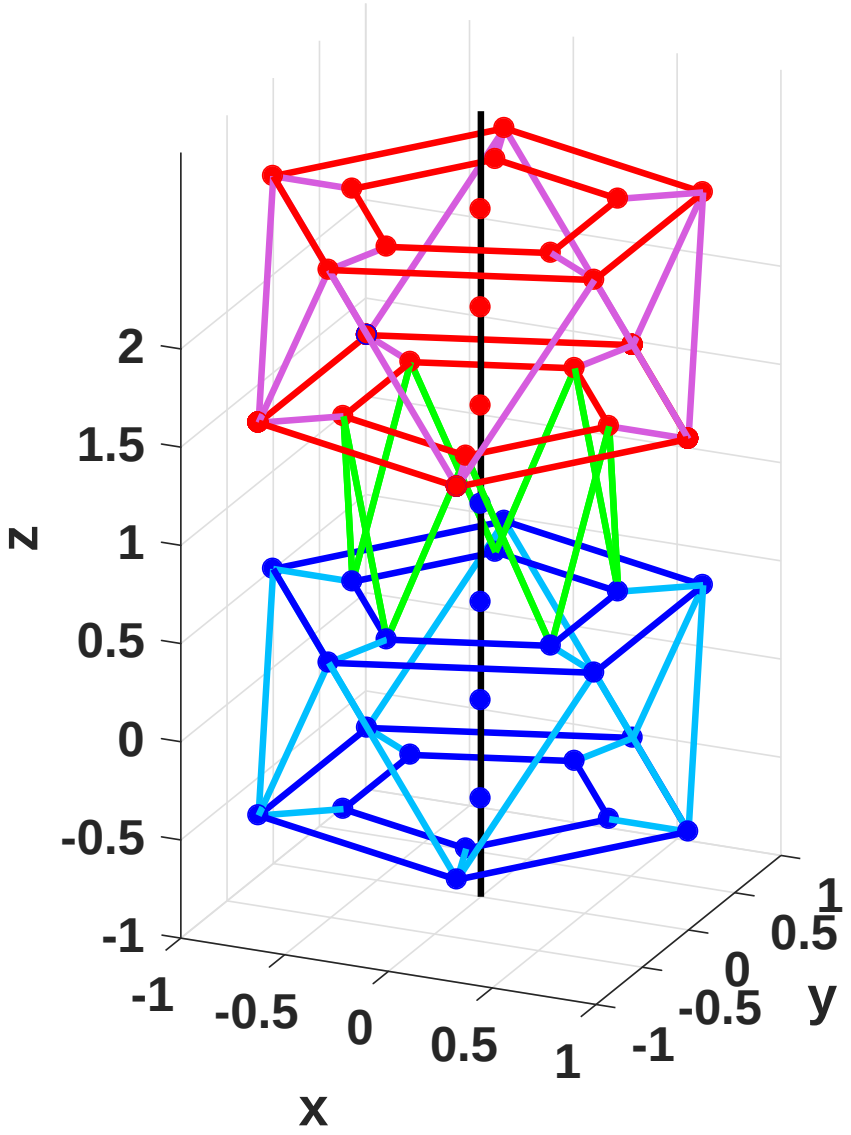

Figure 1: Each RIWV embedded a PPIT translates along $z-axis$ direction forming a PPIT [see green colored lines].

The FTPs of the new model are similar to the EDPs orthogonalizing the 5-fold and the 2-fold rotational axis of corresponding quasicrystals. The chemical composition of the model is given.

This paper has been organized as follows. Section 2 constructs the periodic mathematical model; Section 3 simulates the FTPs of the models; Section. 4 concludes this paper.

2 Constructing Three-Dimensional Periodic Mathematical Model

The fundamental units of the model consists of RIWV and PPIT. There are four lattice points located at the central axis of RIWV and PPIT [see Fig. 1]. In a unit cell, there are two isolated RIWVs and four overlapped RIWVs. Six PPITs are embedded the six RIWVs,respectively. There are eight PPITs surrounding the two isolated RIWVs.

The projection of the model on $x-y$ plan is shown in Fig.2, which is similar to the HREM images obtained by Hiraga et al. from Al-Mn-Si alloy[11] . Therefore the model generated by cubic cells [see Figs. 1-4].

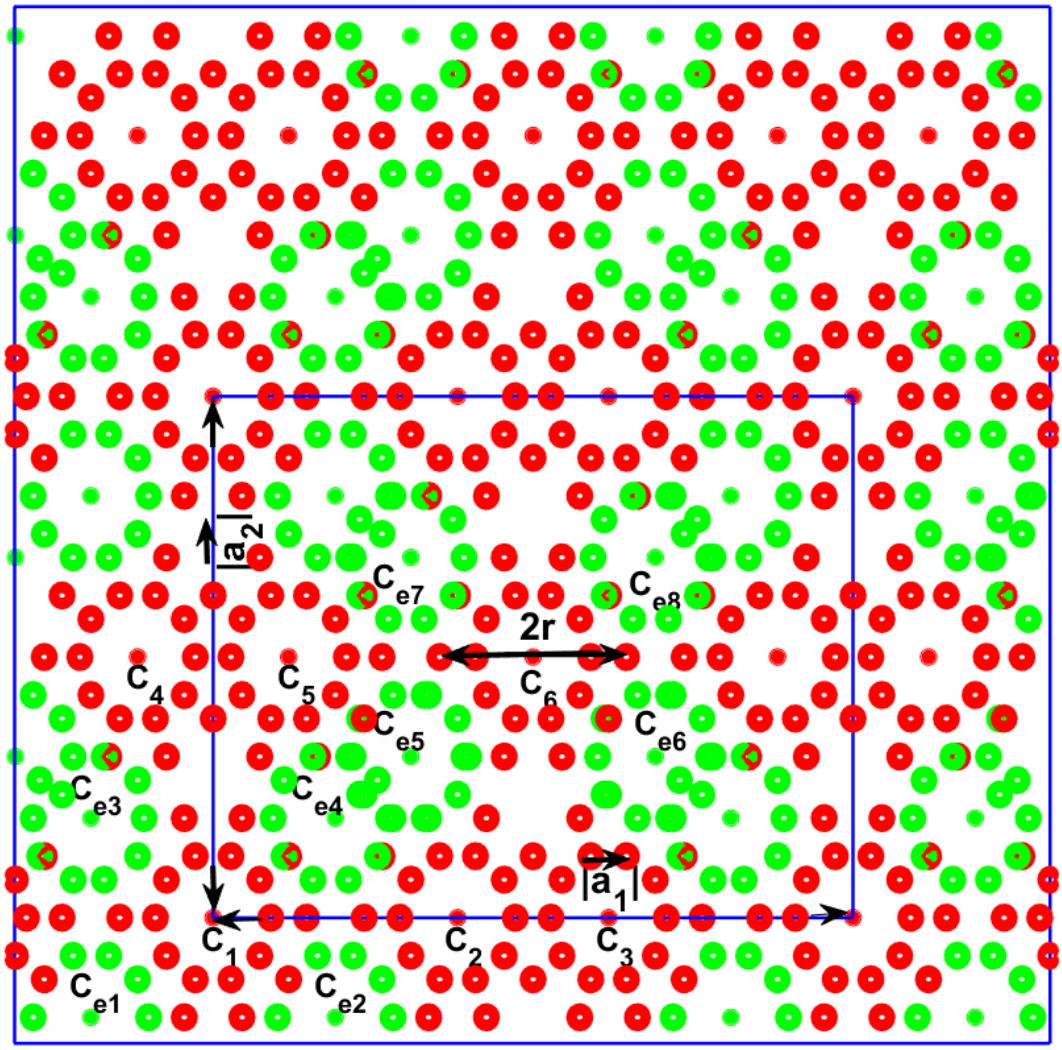

Figure 2: The formed tiling of the projection on $x-y$ plane of the periodic model.

Let r be the radius of the projection circle of the RIWVs [see Fig. 2]. The lengths of the cubic cell are given as follows:

$$|\overrightarrow{\boldsymbol{a}_1}| = r(5+6\sin(\pi/10)), \quad (1)$$

$$|\overrightarrow{\boldsymbol{a}_2}| = 4r(1+\sin(\pi/10))\cos(\pi/10), \quad (2)$$

$$|\overrightarrow{\boldsymbol{a}_3}| = 2r \quad (3)$$

where $\boldsymbol{a}_1$, $\boldsymbol{a}_2$ and $\boldsymbol{a}_3$ are primitive lattice vectors.

The positions of the twenty lattices of an RIWV embedded an PPIT with center at (0, 0, 0) are listed in Table 1. The positions of the four "centers " of an RIWV with center at (0, 0, 0) are given in Table 2.

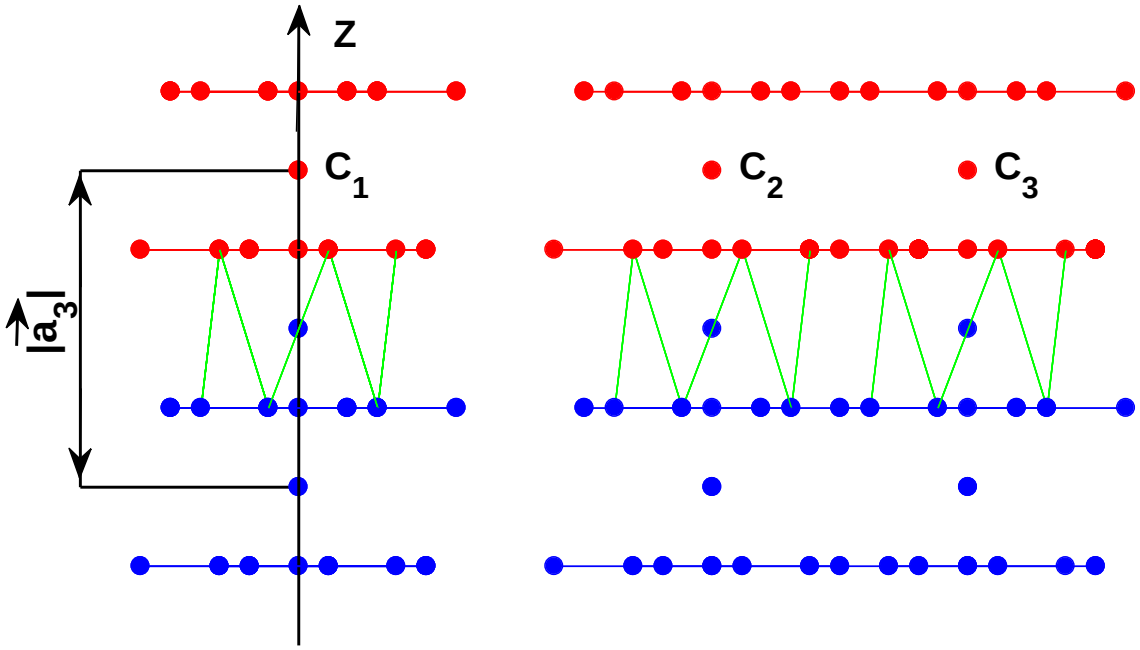

Figure 3: The projection on $x-z$ plane of two isolated RIWVs and four overlapped RIWVs embedded six PPITs, respectively.

Table 1: The positions of the twenty lattices of an RIWV embedded an PPIT with center at (0, 0, 0) where $j = 1, 2, 3, 4, 5$.

i -th type	x_j^i	y_j^i	z_j^i
1	$2r\sin(\pi/10)\cos(72\pi j/180)$	$2r\sin(\pi/10)\sin(72\pi j/180)$	$-r/2$
2	$r\cos(72\pi j/180)$	$r\sin(72\pi j/180)$	$r/2$
3	$r\cos((72\pi j+36)/180)$	$r\sin((72\pi j+36)/180)$	$-r/2$
4	$2r\sin(\pi/10)\cos((72\pi j+36)/180)$	$2r\sin(\pi/10)\sin((72\pi j+36)/180)$	$r/2$

Table 2: The positions of the four "centers " of an RIWV with center at (0, 0, 0).

i -th type	x_0^i	y_0^i	z_0^i
1	0	0	$r/2$
2	0	0	0
3	0	0	$-r/2$
4	0	0	$-r$

That each RIWV translates along $z-axis$ direction forming a new plouhedron. which has the same edge length as PPIT [see Fig.1].

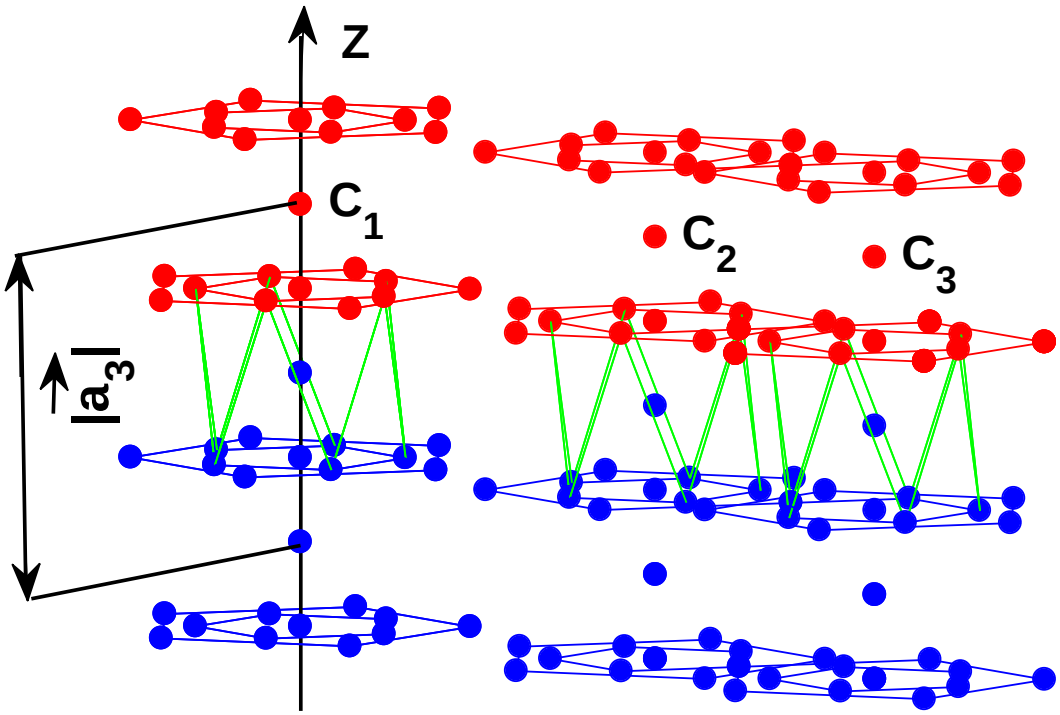

Figure 4: There-dimensional image of two isolated RIWVs and four overlapped RIWVs embedded six PPITs, respectively.

Let C_0^i $(i = 1, 2, \ldots, 6)$ be the centers of the six RIWVs (denoted by $C_j, j = 1, 2, \ldots, 6$) in the a unit primitive cell. C_0^i's can be denoted as follows:

$$\begin{aligned}
C_0^1 &= (0,0,0), && (4)\\
C_0^2 &= (2r(1+\sin(\pi/10)),0,0), && (5)\\
C_0^3 &= C_0^2 + r(1+2\sin(\pi/10)),0,0), && (6)\\
C_0^4 &= (-2r(1+sin(\pi/10))\cos(2\pi/5), 2r(1+sin(pi/10))\sin(2\pi/5,0), && (7)\\
C_0^5 &= C_0^4 + r(1+2\sin(\pi/10)),0,0), && (8)\\
C_0^6 &= C_0^5 + (2r(1+\sin(\pi/10)),0,0). && (9)
\end{aligned}$$

The the positions of the vertices of the mth RIWV embedded mth PPIT can denoted by:

$$C_j^{m,i} = C_0^k + (x_j^i, y_j^i, z_j^i), \quad j = 1,2,3,4,5;\ i = 1,2,3,4; m = 1,2,\ldots,6. \tag{10}$$

Let C_2^i and C_3^i $(m = 1, 2, \ldots, 8)$ be the center positions of the PPIT on $z = r/2$ plan and $z = r/2$ plan. Then these positions have as following forms [see Fig. 3]:

$$\begin{aligned}
C_2^i &= C_0^i + (0,0,r/2), \quad i = 1,2,\ldots,6, && (11)\\
C_3^i &= C_0^i + (0,0,-r/2), \quad i = 1,2,\ldots,6. && (12)
\end{aligned}$$

Let $C'_{em}s$ $(m = 1, 2, \ldots, 8)$ be the center positions of the PPITs on $z = 0$ plan. Let C_{em}^1 and C_{em}^2 be the the centers of the surrounding PPIT on $z = r/2$ plan, and $z = -r/2$ plan. Then these positions have the following forms [see Fig3. 1-3]:

$$C_{e1} = (-2r(1+\sin(\pi/10))\cos(\pi/5), 2r(1+\sin(\pi/10))\sin(\pi/5), 0), \tag{13}$$
$$C_{e2} = (2r(1+\sin(\pi/10)), 0, 0) + C_{e1}, \tag{14}$$
$$C_{e3} = (0, 2r(1+2sin(\pi/10))\sin(\pi//5), 0) + C_{e1} \tag{15}$$
$$C_{e4} = (2r(1+\sin(\pi/10)), 0, 0) + C_{e3} \tag{16}$$
$$C_{e5} = (r(1+2\sin(\pi/10))\cos(\pi/5), r(1+2\sin(\pi/10))\sin(\pi/5), 0) + C_{e4}, \tag{17}$$
$$C_{e6} = (2r(1+\sin(\pi/10)), 0, 0) + C_{e5}, \tag{18}$$
$$C_{e7} = (0, 2r(1+2sin(\pi/10))\sin(\pi//5), 0) + C_{e5} \tag{19}$$
$$C_{e8} = (2r(1+\sin(\pi/10)), 0, 0) + C_{e7} \tag{20}$$

$$C^1_{e1} = C_{e1} + (0, 0, r/2), \tag{21}$$
$$C^1_{e2} = C_{e2} + (0, 0, r/2), \tag{22}$$
$$C^1_{e3} = C_{e3} + (0, 0, r/2), \tag{23}$$
$$C^1_{e4} = C_{e4} + (0, 0, r/2), \tag{24}$$
$$C^3_{e5} = C_{e5} + (0, 0, r/2), \tag{25}$$
$$C^1_{e6} = C_{e6} + (0, 0, r/2), \tag{26}$$
$$C^1_{e7} = C_{e7} + (0, 0, r/2), \tag{27}$$
$$C^1_{e8} = C_{e8} + (0, 0, r/2). \tag{28}$$

$$C^2_{e1} = C_{e1} + (0, 0, -r/2), \tag{29}$$
$$C^2_{e2} = C_{e2} + (0, 0, -r/2), \tag{30}$$
$$C^2_{e3} = C_{e3} + (0, 0, -r/2), \tag{31}$$
$$C^2_{e4} = C_{e4} + (0, 0, -r/2), \tag{32}$$
$$C^2_{e5} = C_{e5} + (0, 0, -r/2), \tag{33}$$
$$C^2_{e6} = C_{e6} + (0, 0, -r/2), \tag{34}$$
$$C^2_{e7} = C_{e7} + (0, 0, -r/2), \tag{35}$$
$$C^2_{e8} = C_{e8} + (0, 0, -r/2). \tag{36}$$

Let C^i_4 and C_{4em} $(i = 1, 2 \ldots, 6) m = 1, 2, \ldots, 8)$ be the center positions of the PPIT at the $z = -r$ plan. Then these positions have as following forms [see Fig. 3]:

$$C^i_4 = C^i_0 + (0, 0, -r), \quad i = 1, 2, \ldots, 6 \tag{37}$$
$$C_{4em} = C_{em} + (0, 0, -r), \quad m = 1, 2, \ldots, 8. \tag{38}$$

The the positions of the vertices of the mth surrounding PPIT can be denoted by:

$$C^{m,i}_{ej} = C_{em} + (x^i_j, y^i_j, z^i_j), \quad j = 1, 2, 3, 4, 5;\ i = 1, 2, 3, 4;\ m = 1, 2, \ldots, 8. \tag{39}$$

In summary, we construct a cubic cells model. In a unit primitive cell, there are 256 atoms. The distances between two atoms located the unit primitive cell are listed as follows [see Fig. 5]:

$$d_0 = 0.5r, \tag{40}$$
$$d_1 = 2r\sin(\pi/10) \approx 0.6180r, \tag{41}$$
$$d_2 = 4r\sin(\pi/10)\sin(\pi/5) \approx 0.7265r, \tag{42}$$
$$d_3 = r, \tag{43}$$
$$d_4 = r\sqrt{8\sin(\pi/10)^2(1-\cos(\pi/5)) + 1} \approx 1.0705r, \tag{44}$$
$$d_5 = r\sqrt{3 - 2\cos(\pi/5)} \approx 1.1756r. \tag{45}$$

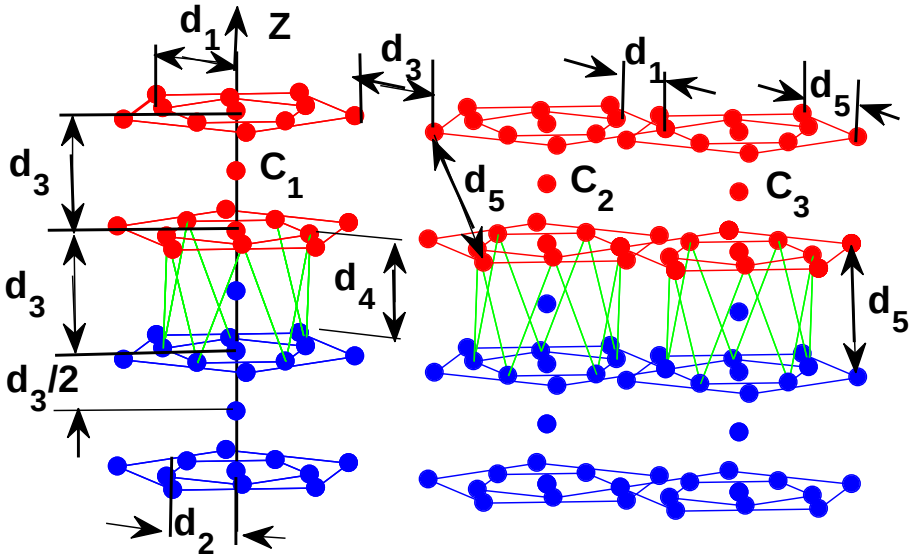

Figure 5: The distances between two neighboring atoms in the model.

3 Fourier-Transform Patterns of the Model

Now we use the primitive lattices vector $\boldsymbol{a}_1$, $\boldsymbol{a}_2$ and $\boldsymbol{a}_3$ to express the coordinates of the atoms defined by (4)–(39).

(1) For the atoms located at the positions defined by (4)-(9)

$$C_0^i = \alpha_{0,i}\mathbf{a}_1 + \beta_{0,i}\mathbf{a}_2 + \gamma_{0,i}\mathbf{a}_3 \quad for \quad 1 \le i \le 6. \tag{46}$$

(2) For the atoms located at the positions defined by (10)

$$C_j^{m,i} = \alpha_j^{m,i}\mathbf{a}_1 + \beta_j^{m,i}\mathbf{a}_2 + \gamma_j^{m,i}\mathbf{a}_3 \quad for \quad 1 \le i \le 4; \quad 1 \le j \le 5, 1 \le m \le 6. \tag{47}$$

(3) For the atoms located at the positions defined by (11)-(12)

$$C_1^i = \alpha_{1,i}\mathbf{a}_1 + \beta_{1,i}\mathbf{a}_2 + \gamma_{1,i}\mathbf{a}_3 \quad for \quad 1 \le i \le 6. \tag{48}$$
$$C_2^i = \alpha_{2,i}\mathbf{a}_1 + \beta_{2,i}\mathbf{a}_2 + \gamma_{2,i}\mathbf{a}_3 \quad for \quad 1 \le i \le 6. \tag{49}$$

(4) For the atoms located at the positions defined by (13)-(20)

$$C_{e,i} = \alpha_{e,i}\mathbf{a}_1 + \beta_{e,i}\mathbf{a}_2 + \gamma_{e,i}\mathbf{a}_3 \quad for \quad 1 \le i \le 8. \tag{50}$$

(5) For the atoms located at the positions defined by (21)-(28)

$$C_{ei}^1 = \alpha_{e,i}^1\mathbf{a}_1 + \beta_{e,i}^1\mathbf{a}_2 + \gamma_{e,i}^1\mathbf{a}_3 \quad for \quad 1 \le i \le 8. \tag{51}$$

(6) For the atoms located at the positions defined by (29)-(36)

$$C_{ei}^2 = \alpha_{e,i}^2 \mathbf{a}_1 + \beta_{e,i}^2 \mathbf{a}_2 + \gamma_{e,i}^2 \mathbf{a}_3 \quad for \quad 1 \leq i \leq 8. \tag{52}$$

(7) For the atoms located at the positions defined by (37)-(38)

$$C_4^i = \alpha_{4,i} \mathbf{a}_1 + \beta_{4,i} \mathbf{a}_2 + \gamma_{4,i} \mathbf{a}_3 \quad for \quad 1 \leq i \leq 6. \tag{53}$$

$$C_{4em} = \alpha_{e,i}^4 \mathbf{a}_1 + \beta_{4,i}^4 \mathbf{a}_2 + \gamma_{e,i}^4 \mathbf{a}_3 \quad for \quad 1 \leq m \leq 8. \tag{54}$$

(8) For the atoms located at the positions defined by (39)

$$C_{ej}^{m,i} = \alpha_{e,j}^{m,i} \mathbf{a}_1 + \beta_{e,j}^{m,i} \mathbf{a}_2 + \gamma_{e,j}^{m,i} \mathbf{a}_3 \quad for \quad 1 \leq i \leq 4; \quad 1 \leq j \leq 5, 1 \leq m \leq 8. \tag{55}$$

Therefore the distribution of atoms in the model can be expressed by the function

$$\begin{aligned}
\rho(\mathbf{r}) \quad = \quad & \sum_{h=-\infty}^{+\infty} \sum_{k=-\infty}^{+\infty} \sum_{l=-\infty}^{+\infty} \Bigg(\sum_{i=1}^{6} f_i \delta(\mathbf{r} - (h + \alpha_{0,i} \mathbf{a}_1) + (k + \beta_{0,i} \mathbf{a}_2) + (l + \gamma_{0,i} \mathbf{a}_3)) + \\
& \sum_{i=1}^{4} \sum_{j=1}^{5} \sum_{m=1}^{6} f_{ijm} \delta(\mathbf{r} - (h + \alpha_j^{m,i} \mathbf{a}_1) + (k + \beta_j^{m,i} \mathbf{a}_2) + (l + \gamma_j^{m,i} \mathbf{a}_3)) + \\
& \sum_{i=1}^{6} \sum_{j=1}^{2} f_{ij} \delta(\mathbf{r} - (h + \alpha_{j,i} \mathbf{a}_1) + (k + \beta_{j,i} \mathbf{a}_2) + (l + \gamma_{j,i} \mathbf{a}_3)) + \\
& \sum_{i=1}^{8} f_{ei} \delta(\mathbf{r} - (h + \alpha_{e,i} \mathbf{a}_1) + (k + \beta_{e,i} \mathbf{a}_2) + (l + \gamma_{e,i} \mathbf{a}_3)) + \\
& \sum_{i=1}^{8} \sum_{j=1}^{2} f_{eij} \delta(\mathbf{r} - (h + \alpha_{e,i}^j \mathbf{a}_1) + (k + \beta_{e,i}^j \mathbf{a}_2) + (l + \gamma_{e,i}^j \mathbf{a}_3)) + \\
& \sum_{i=1}^{6} f_{4i} \delta(\mathbf{r} - (h + \alpha_{4,i} \mathbf{a}_1) + (k + \beta_{4,i} \mathbf{a}_2) + (l + \gamma_{4,i} \mathbf{a}_3)) + \\
& \sum_{i=1}^{8} f_{4ei} \delta(\mathbf{r} - (h + \alpha_{e,i}^4 \mathbf{a}_1) + (k + \beta_{e,i}^4 \mathbf{a}_2) + (l + \gamma_{e,i}^4 \mathbf{a}_3)) + \\
& \sum_{i=1}^{4} \sum_{j=1}^{5} \sum_{m=1}^{8} f_{eijm} \delta(\mathbf{r} - (h + \alpha_{e,j}^{m,i} \mathbf{a}_1) + (k + \beta_{e,j}^{m,i} \mathbf{a}_2) + (l + \gamma_{e,j}^{m,i} \mathbf{a}_3))) \Bigg)
\end{aligned}$$

where f_i, f_{ijm},f_{ij}, f_{eii}, f_{4i}, f_{4ei}, f_{eijm} are the scattering factors of the atoms at the positions C_0^i, $C_j^{m,i}$, C_1^i, C_2^i and C_3^i, $C_{e,i}$, $C_{e,i}^1$, $C_{e,i}^2$, C_4^i, C_{4em} and $C_{ej}^{m,i}$. For sake of simplicity, let the scattering factors equal to one.

The diffraction intensity $I(h,k,l)$ (Fourier-transform pattern) at the reciprocal-lattice point $h\mathbf{a}_1^* + k\mathbf{a}_2^* + l\mathbf{a}_3^*$ is given by

$$I(h,k,l) = \mu \left| \int_\infty^\infty \int_\infty^\infty \int_\infty^\infty \rho(\mathbf{r}) exp(-i(h\mathbf{a}_1^* + k\mathbf{a}_2^* + l\mathbf{a}_3^*)) dx dy dz. \right|^2 \tag{56}$$

where μ is a constant.

$$
\begin{aligned}
I(h,k,l) \;=\; & \mu \Bigg[\Bigg[\sum_{i=1}^{6} f_i \cos(2\pi(h\alpha_{0,i} + k\beta_{0,i} + l\gamma_{0,i})) + \\
& \sum_{i=1}^{4}\sum_{j=1}^{5}\sum_{m=1}^{6} f_{ijm} \cos(2\pi(h\alpha_j^{mi} + k\beta_j^{mi} + l\gamma_j^{mi})) + \\
& \sum_{i=1}^{6}\sum_{j=1}^{2} f_{ij} \cos(2\pi(h\alpha_{j,i} + k\beta_{j,i} + l\gamma_{j,i})) + \\
& \sum_{i=1}^{8} f_{ei} \cos(2\pi(h\alpha_{e,i} + k\beta_{e,i} + l\gamma_{e,i})) + \\
& \sum_{i=1}^{8}\sum_{j=1}^{2} f_{1si} \cos(2\pi(h\alpha_{e,i}^{j} + k\beta_{e,i}^{j} + l\gamma_{2,i}^{j})) + \\
& \sum_{i=1}^{6} f_{4i} \cos(2\pi(h\alpha_{4,i} + k\beta_{4,i} + l\gamma_{4,i})) + \\
& \sum_{i=1}^{8} f_{4ei} \cos(2\pi(h\alpha_{e,i}^{4} + k\beta_{e,i}^{4} + l\gamma_{e,i}^{4})) \; + \\
& \sum_{i=1}^{4}\sum_{j=1}^{5}\sum_{m=1}^{8} f_{eij} \cos(2\pi(h\alpha_{e,j}^{m,i} + k\beta_{e,j}^{m,i} + l\gamma_{e,j}^{m,i})) \Bigg]^2 + \\
& \Bigg[\sum_{i=1}^{6} f_i \sin(2\pi(h\alpha_{0,i} + k\beta_{0,i} + l\gamma_{0,i})) + \\
& \sum_{i=1}^{4}\sum_{j=1}^{5}\sum_{m=1}^{6} f_{ijm} \sin(2\pi(h\alpha_j^{mi} + k\beta_j^{mi} + l\gamma_j^{mi})) + \\
& \sum_{i=1}^{6}\sum_{j=1}^{2} f_{ij} \sin(2\pi(h\alpha_{j,i} + k\beta_{j,i} + l\gamma_{j,i})) + \\
& \sum_{i=1}^{8} f_{ei} \sin(2\pi(h\alpha_{e,i} + k\beta_{e,i} + l\gamma_{e,i})) + \\
& \sum_{i=1}^{8}\sum_{j=1}^{2} f_{1si} \sin(2\pi(h\alpha_{e,i}^{j} + k\beta_{e,i}^{j} + l\gamma_{2,i}^{j})) + \\
& \sum_{i=1}^{6} f_{4i} \sin(2\pi(h\alpha_{4,i} + k\beta_{4,i} + l\gamma_{4,i})) + \\
& \sum_{i=1}^{8} f_{4ei} \sin(2\pi(h\alpha_{e,i}^{4} + k\beta_{e,i}^{4} + l\gamma_{e,i}^{4})) + \\
& \sum_{i=1}^{4}\sum_{j=1}^{5}\sum_{m=1}^{8} f_{eij} \sin(2\pi(h\alpha_{e,j}^{m,i} + k\beta_{e,j}^{m,i} + l\gamma_{e,j}^{m,i})) \Bigg]^2
\end{aligned}
\tag{57}
$$

where let $\mu = 0.0008$, the Fourier-transform patterns of the model along different "symmetry directions" are shown Figs. 6, 8 and 10. Figure 7 shows a typical EDP of a quasicrystal with five-fold rotational symmetry [see [12]]. The diffraction spots [see Figs. 6, 8 and 10] are shown as circles whose diameters are proportional to their intensities; the sports whose intensities are less than $0.05I(0,0,0)$ are omitted. The Fourier-transform patterns are similar to the corresponding EDPs [see Fig. 7, and Fig.1 in Ref. [1]].

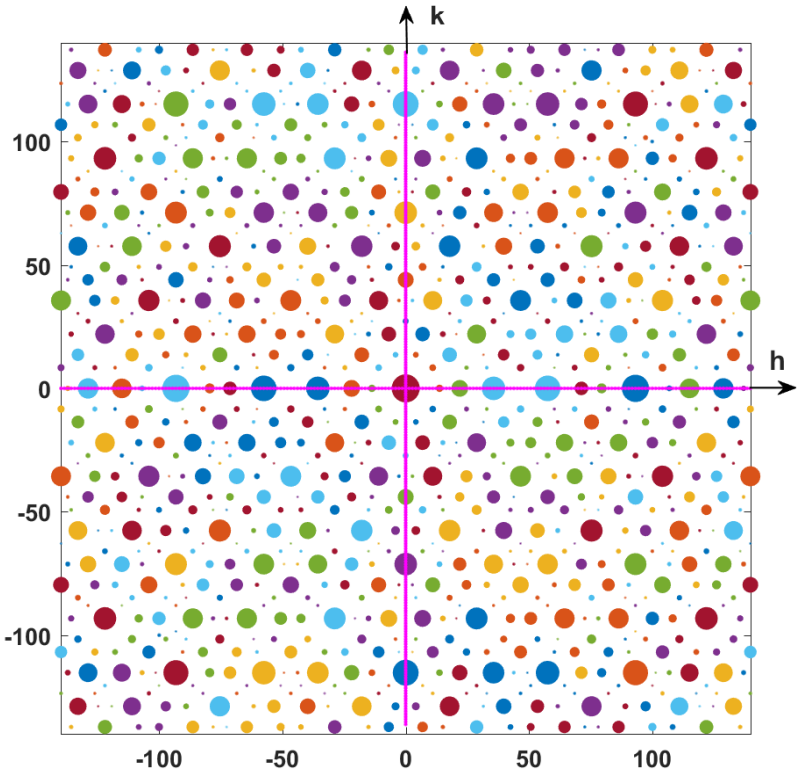

Figure 6: Fourier-transform pattern of the model in a plan orthogonal to a "5-fold symmetry axis".

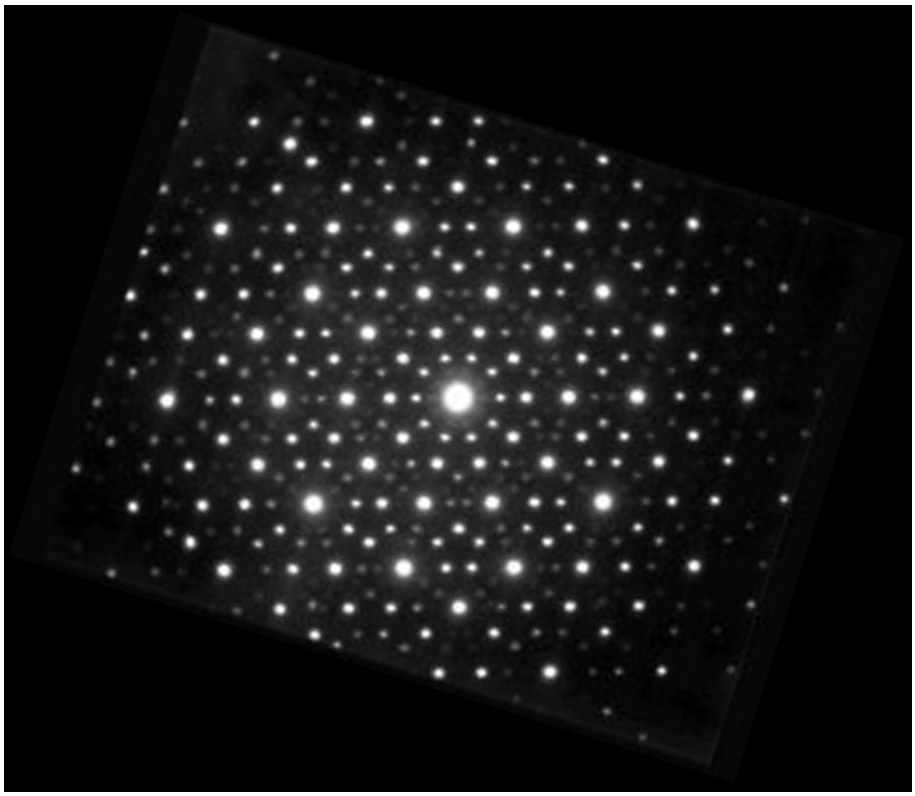

Figure 7: The digitized EDP of a quasicrystal with 5-fold rotational symmetry.

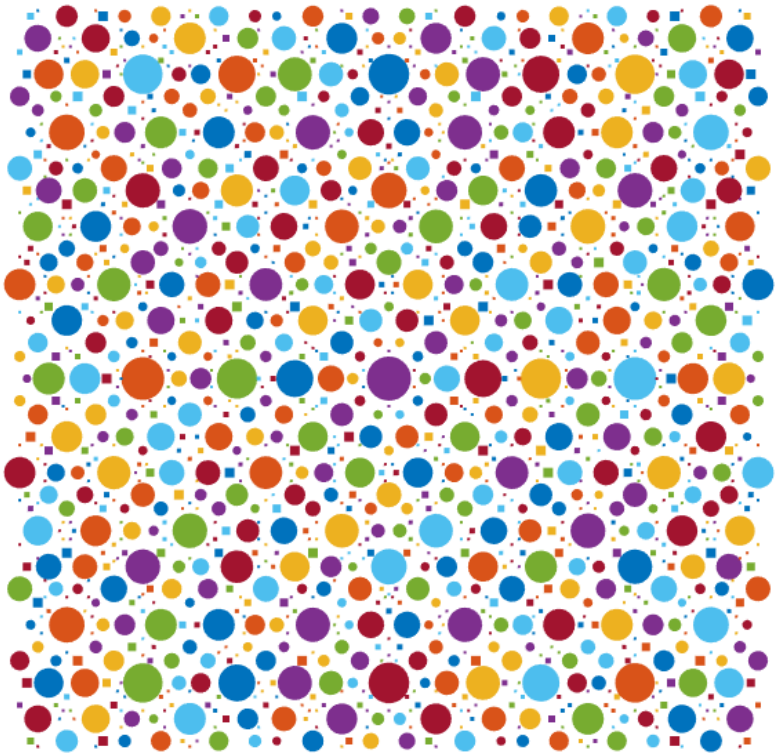

Figure 8: Fourier- transform of the new model in a plan orthogonal to a"5-fold axis" with an angle 63.43^o to $z - axis$.

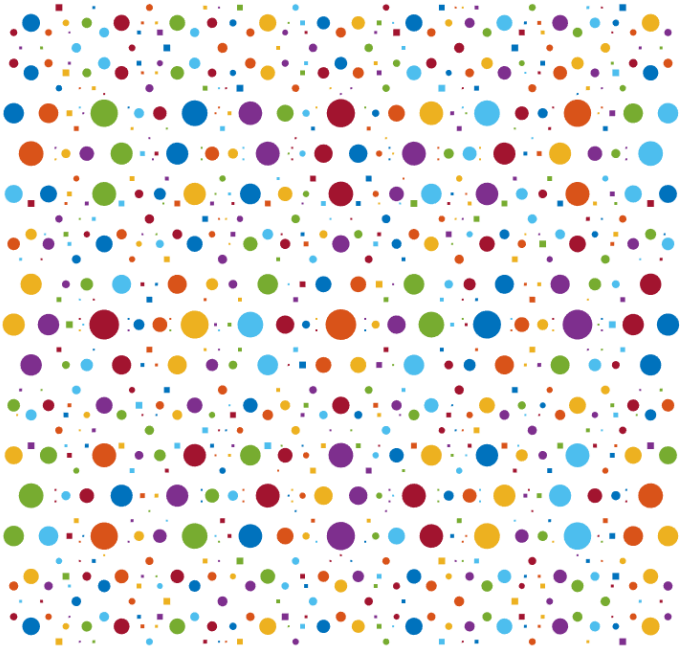

Figure 9: Fourier-transform of the new model in a plan orthogonal to a "2-fold axis" with an angle 32.72^o to $z - axis$.

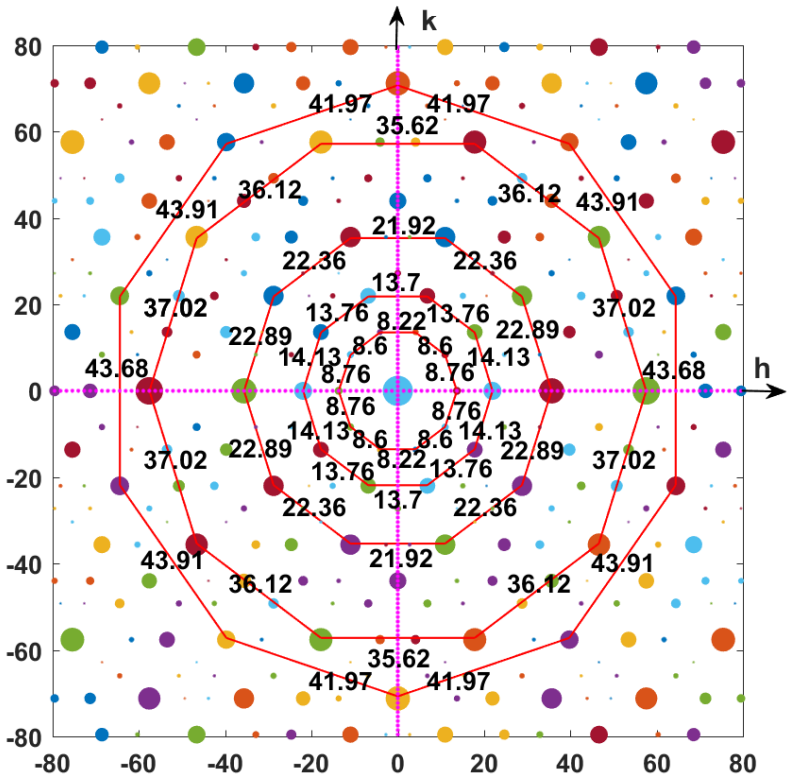

Figure 10: The the distributions of the centers of some FTP circles in Figs. 6 show almost perfect 5-fold rotational symmetry.

In addition, if $r = 6.5\mathring{A}$, then the volume of the unit primitive cell of the model is $44.5517 \times 32.3686 \times 13.0\mathring{A}^3$. Formulas (40)-(45) show that the interatomic distances of the model are between $d_{min} = 0.5r \approx 3.25\mathring{A}$, and $d_{max} \approx 1.1756r \approx 7.6414\mathring{A}$. Furthermore, if the Al atoms at the positions at the "centers" of the 8 surrounding PPITs in a unit primitive cell, and the Mn atoms at the other positions. Then there are 32 Al atoms and 224 Mn atoms in a unit primitive cell. Hence the chemical composition of the model is $Al_{12.5}Mn_{87.5}$ which is very closed to the chemical composition of five fold rotational symmetry quasicrystal [1]. Therefore the atomic structure presented here may be acceptable.

In summary, the presented periodic model can generate the Fourier-transform patterns which are similar to corresponding EDPs of "5-fold symmetry" quasicrystals. The chemical composition of the model is very closed to the chemical composition of the five fold rotational symmetry quasicrystal [1].

If the idealized EDPs of "5-fold symmetry" quasicrystals have 5-fold symmetry in a mathematical sense, then we can conclude that the HREM images of the quasicrystal imply that the quasicrystals are perturbed quasiperiodic structures.

But we can also reasonably assume that the diffraction dots in the idealized EDPs of "5-fold symmetry" quasicrystals are located at corresponding integral lattices points in an orthogonal coordinated systems [see Figs. 6, 8 and 10] which are hardly distinguishable form a pattern with 5-fold symmetry in a strict sense [see Figs. 6, and 10]. This means that the "5-fold symmetry" quasicrystals are essentially crystals but not belong to the classical crystallographic space group because not one of the diffraction patterns of the space group has the approximate "5-fold" symmetry. In this case, we can conclude that the HREM images of the "5-fold symmetry" quasicrystals are perturbed nonclassical crystals.

We prefer the second interpretation since it agrees with the widely held assumption of crystallography and solid state physics– pure solids are either crystalline or glassy.

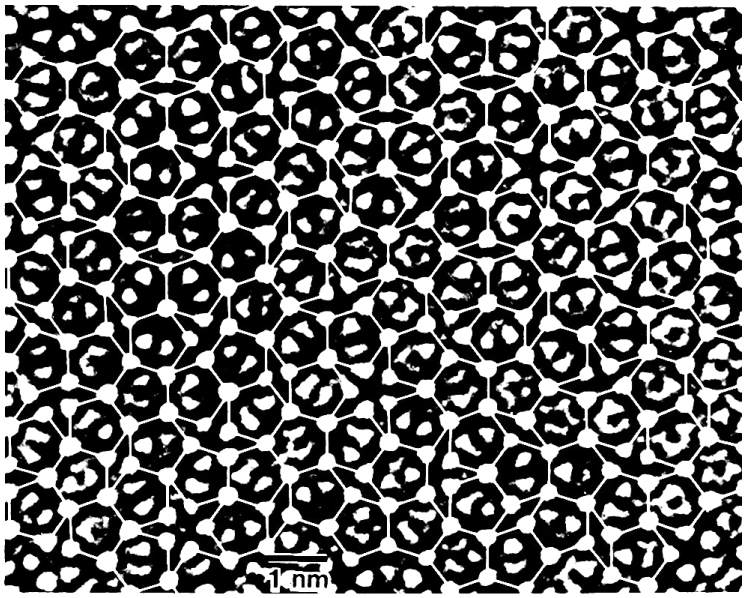

Figure 11: A part of the HREM of the Al-Mn-Si 5-fold quasicrystal reported by Hiraga et al.[11], in which white lines consist of so-called Penrose tiling [Courtesy of K. Hiraga, Tohoku University].

4 Conclusions

Penrose tiling is used widely to describe 5-fold quasicrystals. However it cannot describe the HREM (see Fig. 11) of the AL-Mn-Si 5-fold quasicrystal reported by Hiraga et al.[11]. This study presents one periodic mathematical model based on RIVWs and PPITs. The projections of the model on $x-y$ plan can describe better the HREM [see Fig. 3 and Fig. 11] reported by Hiragaet al.[11] than Penrose tiling. The FTPs and chemical composition of our model is also close to the one of the corresponding 5-fold quasicrystals[1].

Let N denote a three-dimensional lattice point set and let the infimum of the distances between two neighboring lattice points in N be larger than zero. Then for any small enough positive number ε, we can construct an orthogonal (or an oblique) coordinate system A such that for any lattice point (x, y, z) in N, there is an integral lattice point (h, k, l) in A satisfying the condition that the distance between (x, y, z) and (h, k, l) is less than ε. The above fact allows us to believe that the EDPs (Refs. [1, 2, 3, 4, 5]) with fivefold, eightfold, tenfold, and twelvefold symmetries are produced by periodic structures, respectively[8]. Non classical periodic structures are also well candidates to describe quasicrystals. Researches along this line are promising.

Funding

The author has not declared a specific grant for this research from any funding agency in the public, commercial or not for profit sectors.

Conflict of Interest

The author declares no potential conflict of interest.

ORCID iD

Lequan Min http://orcid.org/0000-0002-4414-3818

References

[1] D. Shechtman, I. Blech, D. Dratias, and J. M. Cahn, "Metallic phase with long-rang orietational ordder and no tanslational symetry," *Phys. Rev. Lett.*, vol. 53, pp. 1951–1954, 1984.

[2] N. Wang and K. H. Kuo, "Two-dimensional quasicrystal with eightfold rotational symmetry," *Phys. Rev. Lett.*, vol. 59, p. 1010, 1987.

[3] L. Bendersky, "Quasicrystal with one-dimensional translational symmetry and a tenfold rotation axis," *Phys. Rev. Lett.*, vol. 55, p. 1461, 1985.

[4] T. Ishimasa, H. U. Nissen, and Y. Fukanao, "New ordered state between crystalline and amorphous in ni-cr particles," *Phys. Rev. Lett.*, vol. 55, p. 551, 1985.

[5] H. Chen, D. X. Li, , and K. K. Kuo, "New type of two-dimensional quasicrystal with twelvefold rotational symmetry," *Phys. Rev. Lett.*, vol. 60, p. 1645, 1988.

[6] P. Steinhart and D. Divincenzo, *Quasicrystals: The State of the Art.* Word Scientific, Singapore, 1991.

[7] L. Min and Y. Wu, "Three-dimensional periodicity and twelvefold rotational symmetry," *Phys. Rev. Lett.*, vol. 65, p. 3409, 1990.

[8] ——, "Understanding twelvefold symmetryin electron-diffraction patterns," *Phys. Rev. B*, vol. 45, p. 10306, 1992.

[9] ——, "Reply to "comment on 'understanding twelvefold symmetryin electron-diffraction patterns' "," *Phys. Rev. B*, vol. 49, p. 16052, 1994.

[10] L. Min, "Understanding Fivefold Symmetry in Electron-Diffraction Patterns," Available April 20, 2024, https://www.ChinaXiv.org.

[11] K. M. Hiraga, Hirabayashi, A. Inoue, and T. Masumoto, "Hig-resolution electron microscopy of Al-Min-Si and Al-Mn decagonal quasicrystals," *J. Microscopy*, vol. 146, no. Pt. 43, p. 245, 1987.

[12] Baidu.com, "Electron-diffraction patterns of five fold symmetry quasicrystal," Available May 13, 2024, https://image.baidu.com/search/index?tn=baiduimage&ct=201326592&lm=-1&cl=2&nc=1&ie =utf-8&word=准晶体衍射图.